Inorganic Chemistry

Article

pubs.acs.org/IC

DFT Study of Oxo-Functionalized Pentavalent Dioxouranium Complexes: Structure, Bonding, Ligand Exchange, Dimerization, and U(V)/U(IV) Reduction of OUOH and $OUOSiH_3$ Complexes

Samuel O. Odoh and Georg Schreckenbach*

Department of Chemistry, University of Manitoba, Winnipeg, MB, Canada R3T 2N2

Supporting Information

ABSTRACT: The structural and electronic properties of model oxo-functionalized pentavalent dioxouranium complexes have been studied using scalar relativistic density functional theory (DFT) calculations. The electronic structures of these complexes are compared to those of their hexavalent and pentavalent counterparts with free axial oxo groups while paying particular emphasis on the effect of oxo-functionalization on the formation of binuclear complexes, the U(V)/U(IV) redox potentials, as well as ligand exchange between the axial and equatorial regions of the dioxouranium moiety. The stabilization of the σ(d) orbitals of the UO_2 moiety is one of the major effects of oxo-functionalization. The origin of this effect is the mixing of the σ(d) orbital of the uranyl group with the σ(OH)/σ($OSiH_3$) orbitals of the axial OH/$OSiH_3$ group. The 6p atomic orbitals of the uranium center are mixed to a greater extent with the σ(d) orbital after stabilization caused by oxo-functionalization. The asymmetric nature of the oxo-functionalization has dramatic effects not only on the U−O bond lengths (elongation by up to 0.24 Å) and U−O bond orders (loss of a full bond order) but also on the formation and type of U_2O_4 core found in binuclear complexes. The loss of a full bond order upon oxo-functionalization means the axial U−OH/U−$OSiH_3$ bonds are only slightly stronger than they would be if they were found in the equatorial region of the uranyl moiety. This raises the possibility of ligand exchange between the axial and equatorial regions as well as increasing the stability of the binuclear complexes with butterfly-shaped U_2O_4 cores relative to those with diamond U_2O_4 cores. Reductive oxo-functionalization results in complexes with lower electron density at their U(V) centers in comparison to UO_2^+ complexes. This has dramatic effects on the calculated U(V)/U(IV) redox potentials.

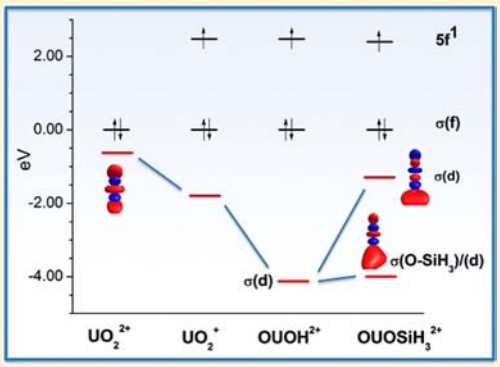

1. INTRODUCTION

There has been a significant resurgence in the synthesis and characterization of various uranium complexes with organic ligands such as macrocycles and expanded porphyrins as well as with inorganic ligands.[1−10] Complexes in which one or both oxo atoms of the uranyl dication have been functionalized with strong Lewis acids such as alkali metals,[11] 3d transition metals,[12] and $B(C_6F_5)_3$[13] have all been reported. In this type of complexes, the +6 oxidation state of the uranium atom is maintained although there is a perturbation of the uranyl group due to the acidic group attached to the axial oxo atoms. The degree to which the uranyl group is perturbed, as evidenced by the change in U═O bond lengths, generally depends on the degree of acidity of the functionalizing group. As examples, functionalization of the uranyl group in Pacman-type complexes by Mn^{2+} and Co^{2+} centers led to U═O bonds that were longer by only 0.010−0.020 Å.[12] This rather small change in bond lengths was reflected in a reduction in the uranyl stretching vibrational frequencies by about 6−10 cm^{-1}. The slight perturbation of the uranyl bonds in these complexes most likely arose from the fact that 3d metals were strongly bound to an amine site of the organic Pacman-type ligand.[12,14] In contrast, oxo-functionalization by the strongly acidic $B(C_6F_5)_3$ group in $OUOB(C_6F_5)_3(NCN)_2$ significantly perturbs the dioxouranium group resulting in a U−OB bond that is about 0.128 Å longer than the terminal U═O bond.[13] Oxo-functionalization also affects the electrochemical properties of uranyl complexes. For example, the effect of oxo-functionalization on U(VI)/U(V) redox potentials has been demonstrated by Arnold and Love et al.[15] and Hayton and Wu.[16] These workers demonstrated that oxo-functionalization shifts the redox potentials of uranyl complexes significantly, often bringing them within ranges that are accessible against the ferrocene/ferrocenium electrode.

On the other hand, there is another class of oxo-functionalized dioxouranium complexes, those in which the oxo-functionalization of an axial oxo atom is accompanied by the transfer of an electron to the U(VI) center. Historically, the pentavalent state of the uranyl moiety is difficult to isolate and characterize in an aqueous environment due to its susceptibility to disproportionation and oxidation.[1,4] Ikeda and co-workers previously used a spectro-electrochemical approach to study uranyl pentavalent complexes by electrochemically reducing

Received: August 10, 2012
Published: December 17, 2012

   dx.doi.org/10.1021/ic301762g | Inorg. Chem. 2013, 52, 245−257

Table 1. Structural Properties and Vibrational Frequencies of the Uranyl Dication and Its Pentavalent Derivatives Obtained at the B3LYP/B1 Level[a]

	bond length (Å)			bond angle (deg)	UO_2 stretching (cm^{-1})	
	U=O	O—X	U—OH_2	O—U—O	sym	asym
			Bare Cations[b]			
UO_2^{2+}	1.698			180.0	1033.7	1126.3
UO_2^{+}	1.760			180.0	924.6	993.3
$OUOH^{2+}$	1.711/1.898	0.993		180.0	774.3	1030.7
$OUO(SiH_3)^{2+}$	1.720/1.849	1.973		180.0	761.6	1022.5
			Pentaaquo Complexes[b]			
$UO_2(H_2O)_5^{2+}$	1.748 (1.76)[c]		2.497 (2.41)[c]	180.0	934.2 (870)[d]	1018.4 (965)[d]
$UO_2(H_2O)_5^{+}$	1.809		2.591	180.0	833.8	889.2
$OUOH(H_2O)_5^{2+}$	1.773/1.990	0.971	2.496–2.528	175.4	673.8	916.4
$OUO(SiH_3)(H_2O)_5^{2+}$	1.776/1.965	1.764	2.511–2.540	176.7	818.2	908.2

[a]X is H and SiH_3 for the oxo-protonated and oxo-silylated pentavalent complexes, respectively. The experimental values are given in parentheses. [b]For the oxo-functionalized complexes, the U—O bonds of the dioxouranium units are given as $U-O_{free}/U-O_{func}$. [c]Reference 83. [d]References 84 and 85.

hexavalent complexes.[17−21] The properties of the quasi-stable pentavalent complexes produced in the optically transparent electrochemical cell were then measured using spectroscopic approaches such as NMR,[18] IR,[20] and extended X-ray absorption fine structure (EXAFS).[17] There has however been significant progress in the synthesis, isolation, and characterization of $U(V)O_2$ complexes since the isolation of a uranyl triphenyl phosphine oxide cation with a triflate anion pair by Berthet et al.[22] Similar works in which chemical reduction of UO_2^{2+} complexes was achieved with cobaltocene, Cp_2Co, have been reported.[16] It should however be noted that a large proportion of reported pentavalent dioxouranium complexes are actually oxo-functionalized complexes in which reduction is achieved simultaneously by conversion of an axial oxo group into an OX-type group (where X is either an alkali metal salt as in the polymeric complexes of Mazzanti's group[23−28] or a proton or silyl group as in the works of Arnold and Love et al.[29,30] and Schnaars et al.[31,32] or a lanthanide ion as in the works of Arnold and Love et al.[33,34]). The polymeric complex initially synthesized by Berthet et al.[35] and Mazzanti et al.[26] has a structure of $([UO_2(py)_5]-[KI_2(py)_2])_\infty$ in which continuous chains of O—U—O are functionalized at both ends by KI_2 groups. These workers have been successful in forming several complexes with tetrameric U_4O_8 cores by reaction of their polymeric salt with various organic ligands.[24,25,27,28] The dioxouranium groups in these tetrameric complexes interact with each other via cation−cation interactions (CCI), in a side-on format leading to an overall square shape.

The ultimate goal of workers involved in the synthesis and characterization of stable oxo-functionalized dioxouranium(V) complexes would be to gain insights into the electronic structure and physical properties of the +5 oxidation state of uranium[1,3,4] as well as into the reduction of U(VI) to U(IV) as an approach to retarding the migration of radionuclides in the environment. The ability of these complexes to form polynuclear species through cation−cation interactions would provide better understanding of these interactions in the complexes of higher actinides, notably Np and Pu. In addition, a better understanding of the structural and electronic properties of pentavalent oxo-functionalized UO_2 complexes could be gained from theoretical calculations. This is due to the fact that computational actinide chemistry has emerged as a useful complement to experimental actinide chemistry over the past few years.[7,36−60] In addition to complementing experimental work, theoretical calculations have also been used by various workers to bridge gaps in our understanding of the chemical properties and speciation of actinide complexes.[47] However, in contrast to extensive studies of UO_2^{2+} and UO_2^{+} complexes with free oxo groups,[61,62] theoretical studies of pentavalent oxo-functionalized dioxouranium complexes are few and far between. $OUOH^{2+}$, the oxo-protonated pentavalent derivative of the uranyl dication, has been studied by several workers.[46,63−66] The interest in this complex arises mainly from its possible role as an intermediate in the quenching of uranyl excited states. An analogous system, NUNH, the oxo-protonated derivative of NUN, a uranyl analogue, was also studied by Wang et al.[67] To further expand our understanding of oxo-functionalized pentavalent complexes in general, we here present a density functional theory (DFT) study of the structural and electronic properties of several oxo-protonated and oxo-silylated pentavalent complexes. In this study of the $OUOX^{2+}$ complexes (X is H or SiH_3), particular emphasis was placed on (1) comparing their electronic structures and structural properties to those of hexavalent and pentavalent species with free oxo groups, (2) comparing the nature of the axial $OH/OSiH_3$ groups to those of equatorial OX groups attached to uranyl groups, (3) examining the possibility of ligand exchange between these axial OX groups and equatorial group, (4) correlating the electronic structure of these complexes to the type of (as well as the ease with which they form) binuclear complexes through cation−cation interactions, and finally (5) determining the influence of oxo-functionalization on the U(V)/U(IV) reduction process.

2. COMPUTATIONAL DETAILS

All DFT calculations in this work were carried out with the Gaussian 03[68] and Priroda[69,70] suites of programs. Tight geometry optimization and energy convergence criteria were stipulated in all the calculations. The evaluation of the exchange-correlation part of the density functionals was carried out with ultrafine grids. The calculation of the harmonic vibrational frequencies allowed for the characterization of the nature of the optimized structures on the potential energy surfaces. In all cases, the vibrational analyses were carried out with the same basis set size and density functional employed in the geometry optimization. Calculations employing relativistic effective core potentials (RECPs) to describe the uranium atoms were carried out with Gaussian 03 while those employing all-electron (AE) basis sets were carried out with the Priroda suite of programs.

dx.doi.org/10.1021/ic301762g | Inorg. Chem. 2013, 52, 245−257

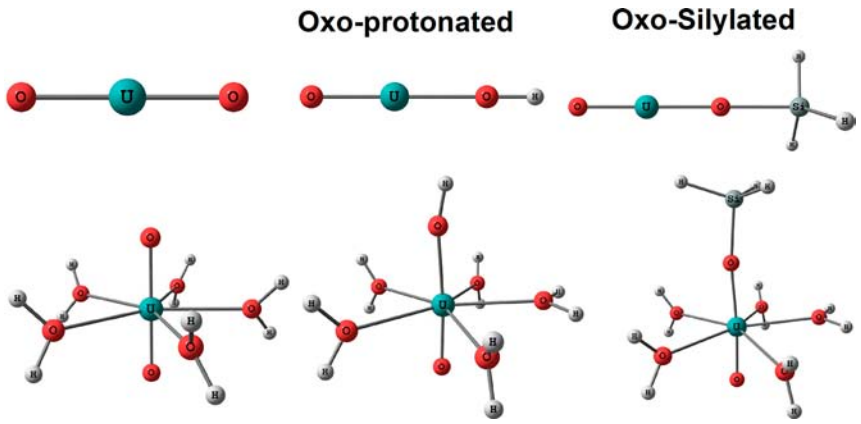

Figure 1. Optimized structures of UO_2^{2+}, $OUOH^{2+}$, and $OUO(SiH_3)^{2+}$ as well as those of their pentaaquo analogues obtained at the B3LYP/B1 level. The structures of UO_2^{+} and $UO_2(H_2O)_5^{+}$ are visually similar to those of their dication analogues.

In the RECP calculations, the Stuttgart small-core scalar-relativistic pseudopotential was used to describe the uranium atoms.[71,72] The pseudopotential was used to represent 60 core electrons in uranium while the remaining 32 electrons were represented by the associated valence basis set. All g-type functions were removed from the valence basis set. The TZVP basis of Schäfer et al.[73] was used to describe all the other atoms in the molecules. The combination of the relativistic pseudopotential for the uranium atoms and the TZVP basis for the nonactinide atoms is labeled as B1. The B3LYP functional was employed in the RECP computations. The molecular orbitals of the complexes studied in this work were obtained at the B3LYP/B1 level and plotted with a contour level of 0.03. The effects of a solvent environment on the calculated ionization potentials were evaluated with single-point calculations on the gas-phase optimized geometries while employing the polarizable continuum solvation (PCM) model.[74] The default atomic radii of the united atom topological model (UA0) in the Gaussian 03 code were used in the calculations. The solvent phase calculations were carried out in tetrahydrofuran using a dielectric constant of 7.58.

To obtain the population based Mayer atomic charges and bond orders,[75] AE calculations were carried out in Priroda while using the geometries optimized at the B3LYP/B1 level. These AE calculations utilized a scalar-relativistic approximation to the full Dirac equation in which all the spin−orbit terms were separated out and neglected. The L2 basis native to Priroda was used on all atoms. This basis is of double-ζ quality for the large component (cc-pVDZ) while the small component was described using appropriate kinetically balanced basis functions.[69] The PBE functional was used in these calculations, and this level is labeled as the PBE/B2 level.

3. RESULTS AND DISCUSSION

3.1. Structures and Molecular Orbitals. The structure of the uranyl dication and its pentavalent derivatives formed by one-electron reduction and by reductive oxo-functionalization of one oxo atom by either a hydrogen atom or a silyl group are presented in Table 1. The optimized structures of UO_2^{2+} and $UO_2(H_2O)_5^{2+}$ obtained at the B3LYP/B1 level are shown in Figure 1. The calculated U═O bond length increases from 1.698 Å in UO_2^{2+} to 1.760 Å in UO_2^{+}. Ikeda et al. have reported experimental evidence for the weakening of the U═O bonds in their electrochemical reduction of UO_2^{2+} complexes.[17,20] This increase in the separation between the uranium and oxo centers can be explained from an electrostatic perspective. In this picture, the extra density caused by the $5f^1$ electron results in greater repulsion between the uranium and oxo centers. Examination of the composition of the molecular orbitals (MOs) found in the valence regions of these systems, Table 2, shows that, while there is little or no change in the description of the σ(d) and π(d) orbitals, the atomic 5f contributions to the σ(f) (from 58% in the dication to 52% in the pentavalent cation) and π(f) orbitals (from 36% in the dication to 27% in the pentavalent cation) are decreased upon one-electron reduction. In addition, comparison of the relative energies of the Kohn−Sham orbitals shows that the σ(d) and π(d) orbitals are stabilized by about 0.81 and 0.52 eV, respectively, relative to the σ(f) orbital upon reduction, Figure 2. It is also important to note that the σ(f) orbitals are the only valence actinyl orbitals with appreciable uranium 6p atomic contributions in UO_2^{2+} and UO_2^{+}. There is a slight increase in the 6p contributions to these orbitals upon reduction, Table 2. All the actinyl valence orbitals in UO_2^{2+} and UO_2^{+} are shown in Figure 3. The explanation of the notation of the valence orbitals as σ(f), σ(d), π(f), and π(d) can be found in modern reviews of actinide chemistry.[61,62]

Table 2. Energies (eV), Descriptions, and Atomic Orbital Compositions of the Valence Actinyl Orbitals of the UO_2^{2+} and UO_2^{+} Obtained at the B3LYP/B1 Level[a]

	energy	description	composition
UO_2^{2+}			
	0.00	σ(f)	58% U-5f; 15% each O-2p; 6% U-6p
	−0.63	σ(d)	14% U-6d; 37% each O-2p
	−0.95	π(f)	36% U-5f; 31% each O-2p; 2% U-6p
	−1.28	π(d)	24% U-6d; 38% each O-2p
UO_2^{+}			
	2.48	$5f^1$	100% U-5f
	0.00	σ(f)	52% U-5f; 18% each O-2p; 9% U-6p
	−1.12	π(f)	27% U-5f; 35% each O-2p; 3% U-6p
	−1.44	σ(d)	15% U-6d; 38% each O-2p
	−1.80	π(d)	23% U-6d; 38% each O-2p

[a]Only the α spin orbitals of UO_2^{+} are shown. The orbital energies are given with respect to the energy of the σ(f) orbital.

The introduction of five equatorial aquo ligands around the UO_2^{2+} and UO_2^{+} moieties results in the elongation of the U═O bonds by about 0.050 Å in both cases, Table 1. The calculations in this work were carried out in the gas phase in comparison to experimental works on the $UO_2(H_2O)_5^{2+}$ complex that were carried out in aqueous solutions. This explains why the U═O and U—OH_2 bonds obtained for this complex deviate from the experimental values by about 0.012 and 0.087 Å, respectively. This correlates well with our recent work on plutonyl aquo-hydroxo complexes where we found

dx.doi.org/10.1021/ic301762g | Inorg. Chem. 2013, 52, 245−257

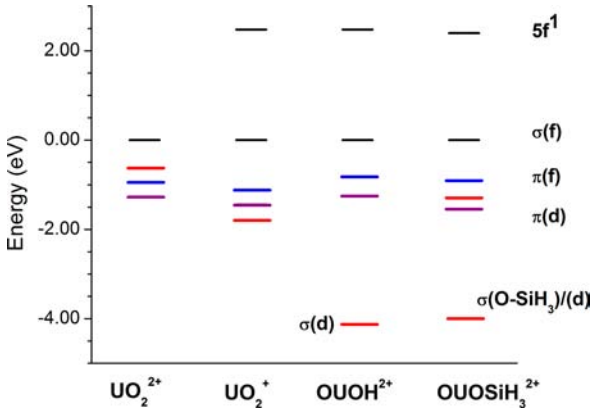

Figure 2. Orbital energy levels of UO_2^{2+}, UO_2^{+}, $OUOH^{2+}$, and $OUO(SiH_3)^{2+}$ obtained at the B3LYP/B1 level. The orbital energies are shifted such that the actinyl σ(f) orbitals are set at 0.00 eV. The σ(d), π(f), and π(d) orbitals are shown with red, blue, and purple bars, respectively. Only the occupied α spin orbital levels of UO_2^{+}, $OUOH^{2+}$, and $OUO(SiH_3)^{2+}$ are shown.

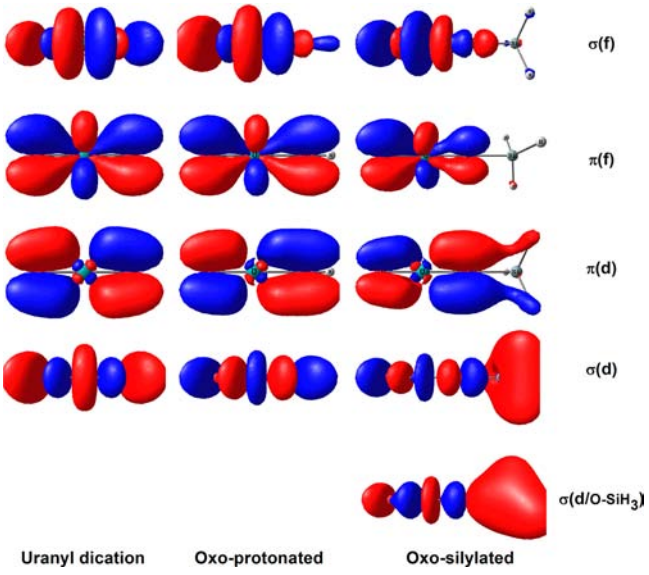

Figure 3. Valence actinyl orbitals of UO_2^{2+}, UO_2^{+}, $OUOH^{2+}$, and $OUO(SiH_3)^{2+}$ obtained at the B3LYP/B1 level. Only the α spin orbitals of the pentavalent complexes are shown.

that the largest impact of an implicit solvation model is in the calculated Pu—OH_2 bond lengths.[47] The optimized structure of $UO_2(H_2O)_5^{2+}$ is shown in Figure 1. For the reduction of $UO_2(H_2O)_5^{2+}$ to $UO_2(H_2O)_5^{+}$, the effect of the weakening of the U═O bonds is the reduction of the calculated frequencies of symmetric and asymmetric uranyl stretching vibrational modes by about 91−100 cm^{-1} and 104−108 cm^{-1}, respectively. The actinyl 5f and 6d atomic contributions to the actinyl orbitals in the pentaaquo complexes, Table 3, are substantially lower than those found in the bare cationic species, Table 2. In contrast, the atomic contributions from the axial oxo atoms remain however mainly constant. In $UO_2(H_2O)_5^{2+}$, the highest occupied orbitals are the oxygen lone pairs of the aquo ligands. Several of these orbitals have some σ(f) and π(f) characters correlating well with some equatorial aquo oxygen 2p character in the σ(f) and π(f) actinyl orbitals. The actinyl σ(f), π(f), σ(d), and π(d) orbitals are found at lower energies than the aquo lone pair orbitals. Below the most stable actinyl orbital, the

Table 3. Energies (eV), Descriptions, and Atomic Orbital Compositions of the Valence Actinyl Orbitals of $UO_2(H_2O)_5^{2+}$ and $UO_2(H_2O)_5^{+}$ Obtained at the B3LYP/B1 Level[a]

	energy	description	composition
$UO_2(H_2O)_5^{2+}$			
	0.00	σ(f)	45% U-5f; 14% each O-2p; 7% U-6p; 3−4% 2p from each OH_2
	−0.76	π(f)	26% U-5f; 32% each O-2p; 3% U-6p
	−0.84	σ(d)	11% U-6d; 38% each O-2p
	−1.33	π(d)	21% U-6d; 37% each O-2p
$UO_2(H_2O)_5^{+}$			
	2.50	$5f^1$	100% U-5f
	0.00	σ(f)	48% U-5f; 20% each O-2p; 10% U-6p
	−0.93	π(f)	22% U-5f; 37% each O-2p; 3% U-6p
	−1.41	σ(d)	12% U-6d; 39% each O-2p
	−1.61	π(d)	22% U-6d; 39% each O-2p

[a]Only the α spin orbitals of $UO_2(H_2O)_5^{+}$ are shown. The orbital energies are given with respect to the energy of the σ(f) orbital.

π(d) orbitals, are several orbitals that are also mainly of oxygen lone pair character on the aquo ligands but with slight uranium 6d (up to 5−6%) contributions. In contrast, for $UO_2(H_2O)_5^{+}$, all the aquo oxygen lone pair orbitals are found below the actinyl valence σ(f), π(f), σ(d), and π(d) orbitals. There are essentially no 5f contributions to the aquo lone pair orbitals, and the 6d contributions are much less than those found in the hexavalent complex. The lack of mixing between the oxygen lone pair orbitals and the actinyl valence orbitals explains why the 5f and 6d contributions to the actinyl orbitals are actually larger in $UO_2(H_2O)_5^{+}$ than in $UO_2(H_2O)_5^{2+}$, Table 3. This also probably contributes to why the U—OH_2 bonds are about 0.094 Å longer in the pentavalent complex. Similar to the case in the bare cations, the U═O bonds are about 0.061 Å longer in the pentavalent complex. Overall, it appears that the lower charge on the U(V) center, compared to the U(VI) center, results in lower electrostatic attraction of the aquo ligands as well as mixing of the actinyl orbitals with the aquo oxygen lone pair orbitals. A similar electrostatics-based explanation is also sufficient for the weakening of the U═O bonds. In the bare cations as well as pentaaquo complexes, the longer U═O bonds formed as a result of one-electron reduction are accompanied by lower frequencies (about 101.0−133.0 cm^{-1} reduction) for the uranyl stretching vibrational modes, Table 1.

The optimized structures of the oxo-protonated and oxo-silylated pentavalent dications as well as those of their pentaaquo analogues are also shown in Figure 1. First, the energy-level diagrams of the valence region of UO_2^{2+}, UO_2^{+}, $OUOH^{2+}$, and $OUO(SiH_3)^{2+}$ are presented in Figure 2. In this figure, the σ(f) orbitals are set at 0.00 eV to allow for easier comparison between these oxo-functionalized pentavalent complexes and the uranyl complexes with free oxo groups. The most noticeable effect of oxo-functionalization is the rather dramatic stabilization of the σ(d) orbital in the oxo-protonated complex. In $OUOH^{2+}$, the σ(d) orbital is found at about 4.14 eV below the σ(f) orbital. This stabilization far exceeds that observed for the reduction of UO_2^{2+} to UO_2^{+}. For the oxo-silylated complex, there are two orbitals with mixed σ(d)/$\sigma(OSiH_3)$ characters. The orbital with greater σ(d) character is found at 1.31 eV below the σ(f) orbital while the one with

dx.doi.org/10.1021/ic301762g | Inorg. Chem. 2013, 52, 245−257

greater $\sigma(OSiH_3)$ character is found at about 4.00 eV below the σ(f) orbital, Figure 2 and Table 4. The σ(d)/$\sigma(OSiH_3)$ orbital at 1.31 eV has about 7% Si-3p contribution while the one at 4.00 eV has negligible contributions from the silyl 3p orbital manifold.

Table 4. Energies (eV), Descriptions, and Atomic Orbital Compositions of the Valence Actinyl Orbitals of $OUOH^{2+}$ and $OUO(SiH_3)^{2+}$ Obtained at the B3LYP/B1 Level[a]

	energy	description	composition
$OUOH^{2+}$			
	2.48	$5f^1$	100% U-5f
	0.00	σ(f)	40% U-5f; 42% O_{free}-2p; 6% U-6p; 4% U-6d
	−0.82	π(f)	25% U-5f; 35% O_{free}-2p; 37% O_{func}-2p
	−1.25	π(d)	19% U-6d; 35% O_{free}-2p; 46% O_{func}-2p
	−4.14	σ(d)	6% U-5f; 7% U-6p; 7% U-6d; 11% O_{free}-2p; 46% O_{func}-2p; 11% H-1s
$OUO(SiH_3)^{2+}$			
	2.39	$5f^1$	100% U-5f
	0.00	σ(f)	46% U-5f; 33% O_{free}-2p; 6% O_{func}-2p; 6% U-6p
	−0.90	π(f)	24% U-5f; 3% U-6d; 53% O_{free}-2p; 17% O_{func}-2p
	−1.31	σ(d)/(O−SiH_3)	8% U-6d; 16% O_{free}-2p; 28% O_{func}-2p; 17% Si-3s; 7% Si-3p
	−1.55	π(d)	17% U-6d; 61% O_{func}-2p; 18% O_{free}-2p
	−4.00	σ(O−SiH_3)/(d)	3% U-6d; 3% U-5f; 3% U-6p; 5% O_{free}-2p; 21% O_{func}-2p; 45% Si-3s; 5% each H-1s

[a]Only the α spin orbitals of these molecules are shown. The orbital energies are given with respect to the energy of the σ(f) orbital.

To trace the origin of the stabilization of the σ(d) orbital in $OUOH^{2+}$, we note that it has been previously shown by us[47] and Ingram et al.[45] that equatorially bonded hydroxo groups stabilize the actinyl σ(d) orbitals below the other actinyl σ and π orbitals. As an example, our calculations show that the σ(d) orbital is about 2.56 eV below the σ(f) orbital in the uranyl hydroxo complex, $UO_2(OH)^+$. This is in contrast to the energy separation of 0.63 eV in UO_2^{2+}. On the other hand, an orbital of mainly σ(O−H) character is found at about 5.36 eV below the σ(f) orbital in $UO_2(OH)^+$. This orbital is shown in Figure 4A. There is about 17% H-1s atomic contribution from the proton of the hydroxo group to this particular orbital. In $OUOH^{2+}$, the σ(d) orbital also contains about 14% H-1s atomic contribution. This suggests that the σ(d) orbital in the oxo-protonated complex is significantly stabilized as a result of mixing with σ(O−H) orbitals. This mixing is allowed due to the axial nature of the OH group, Figure 3. Similarly in $UO_2(OSiH_3)^+$, there exists a $\sigma(OSiH_3)$-type orbital at about 4.93 eV. This orbital contains about 44% 3s atomic contributions from silicon and 5% H-1s contributions from the silyl protons. On going to the oxo-silylated complex, $OUO(SiH_3)^{2+}$, the mixing with the actinyl σ(d) orbitals results in two orbitals, one with predominantly σ(d) character and the other with mainly $\sigma(OSiH_3)$ character, Table 4 and Figure 3. The greater σ-donor character of the hydroxo, in comparison to the siloxo group, is most likely the origin of this discrepancy

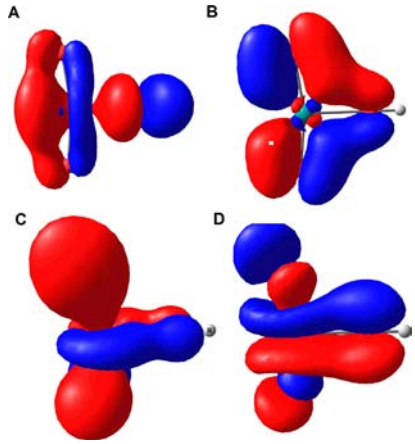

Figure 4. Some molecular orbitals of $UO_2(OH)^+$ with significant U−OH character. (A) HOMO-8 and mainly of mixed σ(O−H)/σ(U−OH) character. It contains 54% 2p from hydroxo oxo atom, 17% H-1s, 9% U-6d, 6% U-5f, 3% U-6p, and 3% 2p from each axial oxo atom. (B) HOMO-7 and mainly of uranyl π(d) character with some π(U−OH) contributions. It contains 33% O-2p from each axial oxo atom, 22% U-6d, and 11% 2p from the hydroxo group. (C) HOMO-4 and mainly of π(f) character with some π(U−OH) contributions. It contains 32% 2p from each axial oxo atom, 27% U-5f, and 5% 2p from the hydroxo group. (D) HOMO-3 and the uranyl σ(f) orbital containing 40% U-5f, 25% 2p from hydroxo, 14% from each axial oxo atom, and 3% U-6p. The composition and shape indicates the presence of significant π(U−OH) character in this orbital.

between the degrees of admixture and stabilization of the σ(d) orbitals (or σ(d)/SiH_3 orbitals for the oxo-silylated system) conferred by both ligands. The stabilization of the σ(d)-type orbitals is also found in the pentaaquo complexes, $OUOH(H_2O)_5^{2+}$ and $OUO(SiH_3)(H_2O)_5^{2+}$. The σ(d) orbital is about 4.76 eV more stable than the σ(f) orbital in $OUOH(H_2O)_5^{2+}$, while similar to the case in $OUO(SiH_3)^{2+}$, the σ(d) and σ(d)/$(OSiH_3)$ orbitals are found at 2.23 and 5.25 eV, respectively, below the σ(f) orbital in $OUO(SiH_3)(H_2O)_5^{2+}$. The mixing of some equatorial σ(O−H)/$\sigma(OSiH_3)$ character into the σ(d) orbitals of the oxo-functionalized complexes is the reason why we considered the influence of equatorial groups on the uranyl moiety in $UO_2(OH)^+$ and $UO_2(OSiH_3)^+$. This is also why we compare the axial and equatorial U−O bond orders in a later section.

It is also interesting to note that the percent contribution of actinide 6p atomic orbitals to the stabilized σ(d) orbitals is increased in the oxo-functionalized complexes. While there are no 6p contributions to the σ(d) orbitals in UO_2^{2+} and UO_2^+, Table 2, oxo-protonation increases the 6p contribution to this orbital to about 7%. Similarly, the 6p participation in the σ(O−SiH_3)/(d) increases slightly to 3%, Table 4. It appears that stabilization of the σ(d) orbitals in the pentavalent oxo-functionalized complexes brings them nearer the semicore/semivalent region allowing for increased mixing with the 6p orbitals. To support this explanation of the increased 6p contributions to the σ(d) orbitals, we note that the semicore/semivalent σ(O−H) orbital, Figure 4A, of $UO_2(OH)^+$ also has 6p contributions of about 3%.

Examination of the atomic contributions to the actinyl valence orbitals in the oxo-functionalized pentavalent complexes reveals significant asymmetry between the contributions of the axial oxo atoms to the σ(d), σ(f), π(d), and π(f) orbitals, Table 4. This contrasts with the equal contributions from these

dx.doi.org/10.1021/ic301762g | Inorg. Chem. 2013, 52, 245−257

Table 5. Calculated Mayer Bond Orders for the U—O, U—OX, and U—OH_2 Bonds in Several Hexavalent, Pentavalent, and Oxo-Functionalized Pentavalent Complexes Obtained at the PBE/L1 Level

	complex	axial bond		equatorial bond	
		U═O/U—O_{free}	U—OX	U—OH_2	U—OH/SiH_3
Hexavalent					
	UO_2^{2+}	2.54			
	$UO_2(OH)^+$	2.48			1.52
	$UO_2(OSiH_3)^+$	2.47			1.51
	$UO_2(H_2O)_5^{2+}$	2.44		0.46	
	$UO_2(H_2O)_4(OH)^+$	2.41		0.36−0.39	1.35
	$UO_2(H_2O)_4(OSiH_3)^+$	2.41		0.37−0.38	1.23
Pentavalent					
	UO_2^+	2.48			
	$UO_2(H_2O)_5^+$	2.42		0.37	
Oxo-Functionalized Pentavalent					
	$OUOH^{2+}$	2.58	1.66		
	$OUO(SiH_3)^{2+}$	2.55	1.89		
	$OUOH(H_2O)_5^{2+}$	2.51	1.46	0.42−0.45	
	$OUO(SiH_3)(H_2O)_5^{2+}$	2.50	1.49	0.41−0.43	

atoms in UO_2^{2+} and UO_2^+ and correlates well with the asymmetric nature of the oxo-functionalization. The atomic 2p contributions of the free oxo atom, O_{free}, dominate in the σ(f) orbitals while the contributions of the functionalized oxo atom, O_{func}, dominate for the σ(d) and π(d) orbitals of the oxo-functionalized complexes, Table 4. The asymmetric contributions from the oxo atoms, which can be visually seen in the orbitals, Figure 3, correlates with the calculated U−O_{free} and U−O_{func} bond lengths in $OUOH^{2+}$ and $OUO(SiH_3)^{2+}$, Table 1. The increased oxygen 2p atomic contributions of the free oxo atom to the σ(f) orbitals of the functionalized oxo atom to the σ(d) and π(d) orbitals as well as the different lengths for the U−O_{free} and U−O_{func} bonds are also seen in the pentaaquo complexes, Tables 1 and 4.

Overall reductive oxo-functionalization increases the U—O bonds by about 0.013−0.030 Å for the free oxo atoms and by 0.151−0.242 Å for the functionalized oxo atoms, Table 1. This contrasts with the calculated elongation of about 0.061 Å obtained for the U═O bonds on moving from UO_2^{2+} to UO_2^+ and from $UO_2(H_2O)_5^{2+}$ to $UO_2(H_2O)_5^+$. The calculated frequencies of the U—O stretching in the oxo-functionalized complexes reflect the asymmetric nature of the U—O_{free} and U—O_{func} bonds. As a result of their asymmetric nature, the asymmetric and symmetric stretching modes associated with the U—O bonds of the dioxouranium unit have mostly been decoupled in the oxo-functionalized complexes. As such these two modes can be more aptly called the U—O_{free} and UO_{func}—X (where X is H and SiH_3 for the oxo-protonated and oxo-silylated complexes) stretching modes, respectively. The U—O_{free} bonds are significantly shorter than the U—O_{func} bonds, agreeing well with the larger vibrational frequencies for the U—O_{free} stretching mode compared to those of the UO_{func}—X stretching modes, Table 1. In addition, we note that the U═O bonds in the pentavalent complexes UO_2^+ and $UO_2(H_2O)_5^+$ are longer than the U—O_{free} bonds in the oxo-functionalized pentavalent complexes. This explains why the frequencies of the asymmetric/U—O_{free} stretching mode are larger than those of the asymmetric stretching modes in UO_2^+ and $UO_2(H_2O)_5^+$, Table 1.

It is also important to mention the relative intensities of the U−O_{free} and UO_{func}−X stretching modes in the oxo-functionalized pentavalent complexes. Unlike in the uranyl complexes, where the asymmetric and symmetric stretching modes are IR and Raman active, respectively, the two modes associated with the dioxouranium unit in the OUOX complexes are both IR active. Essentially, the inherent asymmetry in these complexes breaks the symmetry selection rules allowing for IR activity. Wang et al. have previously reported this in their DFT and experimental work on NUNH.[67] Additional experimental verification of this effect has been reported by Arnold and Love et al. who observed two UO stretching modes in their Nujol mull measurements of several oxo-silylated species.[30]

The energy separations between the σ(f) orbital and the singly occupied $5f^1$ orbital levels in UO_2^+, $OUOH^{2+}$, and $OUO(SiH_3)^{2+}$ are essentially the same, Figure 2. This is in a way a reflection of the atomic nature of the 5f unpaired electron. In addition, the splitting between the $5f^1$ orbital level and the lowest unoccupied molecular orbital (LUMO) was calculated as 3.70, 3.70, and 3.40 eV for UO_2^+, $OUOH^{2+}$, and $OUO(SiH_3)^{2+}$, respectively, at the B3LYP/B1 level. For the pentaaquo complexes, the $5f^1$−LUMO energy gaps were calculated as 3.65, 3.76, and 3.76 eV, respectively. These suggest that the f−f transitions in the electronic spectra of these complexes would be found at similar wavelengths. It should however be noted that spin−orbit coupling effects were neglected in this work.

3.2. Bond Orders. The calculated Mayer bond orders of the U—O bonds in several hexavalent, pentavalent, and oxo-functionalized pentavalent dioxouranium complexes are presented in Table 5. The calculated bond orders for the U═O bonds in UO_2^{2+} and $UO_2(H_2O)_5^{2+}$ are 2.54 and 2.44, respectively. These bond orders are greater than two, an indication of a complete double bond as well as significant triple bond characters. The coordination of either an hydroxo or siloxo group to the uranyl moiety, as in $UO_2(OH)^+$ and $UO_2(OSiH_3)^+$, results in elongation of the U═O bonds. The weakening of these bonds correlates well with the decrease in the bond orders from 2.54 to 2.48 and 2.47 for the hexavalent hydroxide and siloxide species, respectively, Table 5. A similar case is also found in the pentaaquo hydroxide and siloxide complexes. The effect of progressively longer An=O bonds as more anionic ligands are coordinated to actinyl groups has been observed in a large number of cases, uranyl hydroxides,[45,49,76] uranyl fluorides,[50,77] and plutonyl hydroxides[47] being a few

dx.doi.org/10.1021/ic301762g | Inorg. Chem. 2013, 52, 245−257

Table 6. Calculated Structural Parameters of $OUOH(OH)_3(OSiH_3)^{2-}$ and $OUOSiH_3(OH)_4^{2-}$ Obtained at the B3LYP/B1 Level[a]

		axial		equatorial	
	U═O	U—OH	U—$OSiH_3$	U—OH	U—$OSiH_3$
Hexavalent					
trans-$UO_2(OH)_4^{2-}$	1.850 (2.32)			2.305 (1.08)	
cis-$UO_2(OH)_4^{2-}$	1.898 (2.36)	2.264 (1.14)		2.303 (1.08)	
Oxo-Functionalized Pentavalent					
$OUOH(OH)_3(OSiH_3)^{2-}$	1.894 (2.38)	2.203 (1.19)		2.268/2.288 (1.10−1.13)	2.370 (0.62)
$OUOSiH_3(OH)_4^{2-}$	1.894 (2.36)		2.327 (0.70)	2.260−2.278 (1.10−1.13)	

[a]The Mayer bond orders obtained at the PBE/B2 level are given in parentheses.

examples. For the uranyl complexes with equatorial hydroxo and siloxo groups, the U═O bond length increases, and the calculated bond orders for this bond decrease as more ligands are coordinated to the uranyl moiety. The transfer of 5f and 6d electron density from the axial U═O bonds to the equatorial ligands is responsible for this phenomenon. As an example, the U═O bond order continuously decreases until it reaches 2.32 in the terminal hydroxide complex, $UO_2(OH)_4^{2-}$, Table 6.

For UO_2^+, the decrease in the uranium 5f contributions to the σ(f) and π(f) orbitals as well as the repulsion between the unpaired 5f electron and the axial O^{2-} groups, Table 2, are responsible for the weakening of the U═O bonds. This decrease in the covalency of the U═O bonds as well as increased electrostatic repulsion is reflected in the calculated bond orders that decrease from 2.54 to 2.48 for the bare uranyl species. As we noted for $UO_2(H_2O)_5^{2+}$ and $UO_2(H_2O)_5^+$, the 5f contributions to the σ(f) and π(f) orbitals are actually higher in the pentavalent complex. This was explained as due to the absence of mixing with aquo oxygen lone pair type orbitals in the pentavalent species, as opposed to its presence in the hexavalent species. The Mayer bond order, a reflection of covalency, for the U═O bonds actually only decreases slightly from 2.44 in $UO_2(H_2O)_5^{2+}$ to 2.42 in $UO_2(H_2O)_5^+$, further buttressing the role of electrostatic repulsion in the weakening of the axial bonds, Table 5.

The bond orders obtained for the U—O_{free} bonds in $OUOH^{2+}$ and $OUO(SiH_3)^{2+}$ are 2.58 and 2.55, respectively. These values exceed those obtained for UO_2^{2+}, 2.54, and UO_2^+, 2.48. In a similar manner, the calculated bond order of the U—O_{free} bonds in the pentaaquo oxo-functionalized complexes also exceed those of the U═O bonds in their hexa- and pentavalent counterparts with free axial oxo groups, Table 5. For example, the U═O bond order in $UO_2(H_2O)_5^{2+}$ was calculated as 2.44, while it was found to be 2.51 and 2.50 after reductive oxo-protonation and oxo-silylation, respectively. Although this is seemingly in contrast to the previously noted elongation of the U═O bonds by about 0.013−0.030 Å upon oxo-functionalization, Table 1, the decomposition of the valence orbitals in Tables 2 and 4 show that the σ(f) and π(f) orbitals actually contain increased atomic actinide 5f and 2p contributions from the free oxo atom. This greater overlap of the 5f and 2p orbitals, greater covalency, is responsible for the larger bond orders.

The calculated bond orders of the U—O_{func} bonds in the oxo-functionalized pentavalent complexes are between 1.46 and 1.89, Table 5. These represent a reduction of about 0.65−1.08, the loss of nearly a full bond, compared to the U═O bonds in UO_2^{2+} and $UO_2(H_2O)_5^{2+}$. The U—O_{func} bonds are now full single bonds with significant double bond character. In our view, it would be interesting to compare the degree of double-bond character present in the U—O_{func} bonds of these complexes to those found in equatorial U—O bonds in hexavalent uranyl complexes. As examples, the bond orders obtained for the equatorial U—OH and U—$OSiH_3$ bonds are about 1.51−1.52 in $UO_2(OH)^+$ and $UO_2(OSiH_3)^+$, about 1.35 in $UO_2(H_2O)_4(OH)^+$, and 1.23 in $UO_2(H_2O)_4(OSiH_3)^+$, Table 5. These equatorial U—OH/U—$OSiH_3$ bonds in these complexes therefore possess appreciable double-bond characters due to the π-donating abilities of the hydroxo and siloxo ligands. The double-bond characters in these bonds are supported by the presence of orbitals with π(U—OH) characters in the electronic structure of $UO_2(OH)^+$, Figure 4B−D. The mixture of some uranium 5f and 6d orbitals from the U═O bonds, especially from the actinyl σ(f) orbital, into the π(U—OH) framework is responsible for the weakening of the U═O bonds as well as the unusually strong U—OH bonds. This was found to be the case in our recent work on plutonyl hydroxides.[47] Comparison of the calculated bond orders of the U—O_{func} bonds in the pentavalent oxo-functionalized complexes to those obtained for the U—OH and U—$OSiH_3$ bonds in $UO_2(OH)^+$, $UO_2(OSiH_3)^+$, $UO_2(H_2O)_4(OH)^+$, and $UO_2(H_2O)_4(OSiH_3)^+$ show that the axial U—O_{func} bonds are actually only slightly stronger than the equatorial U—OH and U—$OSiH_3$ bonds, Table 5.

3.3. Implications of the Weak U−O_{func} Bonds.

3.3.1. Axial−Equatorial Ligand Stereoisomers. To briefly recap, the major structural effect of oxo-functionalization is the significant weakening of the U−O_{func} bonds. As calculated by the Mayer bond orders, these bonds are only slightly stronger than equatorial bonds between the uranyl moiety and hydroxo/siloxo ligands. This fact implies that "exchange" of the axial OX groups with equatorial groups should be thermochemically facile whenever OX has identical π-donating capabilities as the equatorial group. An example regarding the exchange between equatorial hydroxo groups and axial siloxo groups is given in Figure 5. We note that we are referring to two stereoisomers rather than the "classical" ligand exchange observed by Clark and Grenthe's groups.[78,79] Given that the hydroxo group is a slightly stronger π donor than the siloxo group, one would expect $OUOSiH_3(OH)_4^{2-}$ (axial siloxo group, equatorial hydroxo group) and $OUOH(OH)_3(OSiH_3)^{2-}$ (equatorial siloxo group, axial hydroxo group) to be closer in energy than the structures of $UO_2(OH)_4^{2-}$ with a linear (two axial oxo groups) or bent dioxouranium unit (axial oxo group and axial hydroxo group), Figure 5. We are in essence examining the influence of reductive oxo-silylation on the relative positions of the hydroxo groups in $UO_2(OH)_4^{2-}$. These kinds of stereoisomers can probably be monitored experimentally with isotope labeling techniques.[31]

dx.doi.org/10.1021/ic301762g | Inorg. Chem. 2013, 52, 245−257

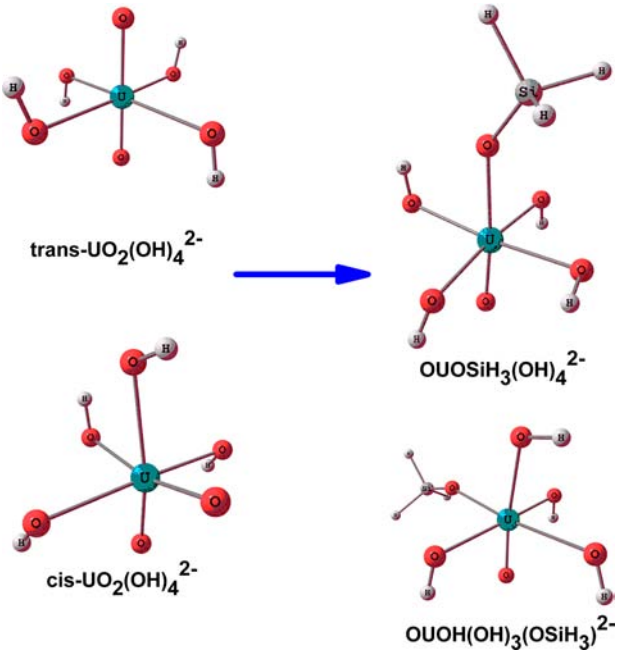

Figure 5. Effect of reductive oxo-silylation on the positions of the hydroxo ligands of $UO_2(OH)_4^{2-}$. The exchange of hydroxo-siloxo ligands between the axial and equatorial positions interconvert $OUOSiH_3(OH)_4^{2-}$ and $OUOH(OH)_3(OSiH_3)^{2-}$.

Starting from the hexavalent complex, the structures of $UO_2(OH)_4^{2-}$ with *trans*- and *cis*-uranyl groups are shown in Figure 5. The exchange of an axial oxo atom with an equatorial hydroxo group in $UO_2(OH)_4^{2-}$ has been studied by several workers.[7,41,52] The structure with a linear dioxouranium unit, the *trans*-uranyl isomer, was found by Schreckenbach et al. to be about 18.0 kcal/mol more stable than the structure with a bent UO_2 group, the *cis*-uranyl isomer.[52] At the B3LYP/B1 level of theory employed in this work, the trans isomer of $UO_2(OH)_4^{2-}$ is about 17.3 kcal/mol more stable than its *cis*-uranyl counterpart. The *cis*-uranyl structure has two O═U—OH units in contrast to the O═U═O unit found in its *trans*-uranyl counterpart. Subsequent to oxo-silylation, we compare O═U—$OSiH_3$ in $OUOSiH_3(OH)_4^{2-}$ to O═U—OH in $OUOH(OH)_3(OSiH_3)^2$. These two complexes are cis and trans isomers of $UO(OSiH_3)(OH)_4^{2-}$, respectively. The lowest energy structures obtained for $OUOSiH_3(OH)_4^{2-}$ and $OUOH(OH)_3(OSiH_3)^{2-}$ are shown in Figure 5. Other structures corresponding to the different orientations of the terminal hydrogen atoms of the silyl and hydroxo groups were also optimized. The energy difference between these structures was found to be only 3.90 kcal/mol, with $OUOH(OH)_3(OSiH_3)^{2-}$ more stable than $OUOSiH_3(OH)_4^{2-}$. This is significantly smaller than the energy difference found between *trans*- and *cis*-$UO_2(OH)_4^{2-}$ and is a reflection of the closer similarity between the siloxo and hydroxo species found in the oxo-functionalized complexes, Table 6. The reduction in the bond order of the axial U═O bond after oxo-functionalization essentially lowers the energy required to exchange the equatorial hydroxo and axial siloxo groups.

The possibility of experimentally observing the existence of two conformers for oxo-functionalized pentavalent species or this kind of exchange between equatorial ligands and axial functionalized oxo groups is an interesting question. To allow for near degeneracy between the two conformers, the bonds formed by the axial functionalized oxo and equatorial ligands with the uranium center must be of similar strength. The relative sizes of these ligands are also an important factor as the ligand exchange step leading to the formation of a new conformer would be expected to be slower for bulky ligands. Although, we know of no experimental observation of exactly this kind of exchange reaction, we find the observation of conformers corresponding to "axial−equatorial" ligand exchange in $U(OSiPh_3)(OB[C_6F_5]_3)(^{Ar}acnac)_2$ and $U(OSiEt_3)_2(^{Ar}acnac)_2$ by Schnaars et al. rather tantalizing.[31,32] In contrast to the complexes studied in the current work, the pentavalent complexes studied by Schnaars et al. are doubly oxo-functionalized.[31,32]

Examination of the calculated structural parameters obtained for $OUOH(OH)_3(OSiH_3)^{2-}$ and $OUOSiH_3(OH)_4^{2-}$ at the B3LYP/B1 level shows that the axial U—OH and U—$OSiH_3$ bonds, which are trans to the oxo group, are about 0.060 and 0.043 Å shorter than their equatorial counterparts, respectively, Table 6. This inverse trans effect results in the strengthening of the bonds that are trans to the strongly bound O^{2-} ligand of the U═O moiety and is supported by the larger bond order of 1.19 for the axial U—OH bond in $OUOH(OH)_3(OSiH_3)^{2-}$ compared to 1.10−1.13 for the equatorial U—OH bonds. A similar case is observed for the conformers of $UO_2(OH)_4^{2-}$ with *cis*- and *trans*-uranyl groups, Table 6.

3.3.2. Stability and Structure of Bis(dioxouranium) Complexes. A substantial fraction of the stable U(V) complexes that have been experimentally synthesized and characterized contain cation−cation type interactions between two or more UO_2 species.[1,4,27,28,35] There are generally two structural motifs for cation−cation interactions in binuclear U(V) complexes: the diamond motif in which the two uranyl groups are in (nearly) parallel arrangement and the aptly named T-shaped motif in which the uranyl groups are (nearly) perpendicular, Figure 6. On the other hand, U(V) complexes featuring a

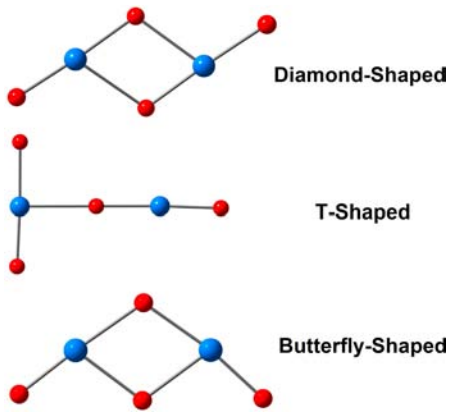

Figure 6. Diamond-, T-, and butterfly-shaped frameworks of the U_2O_4 core found in bis(dioxouranium) systems. The uranium and oxygen atoms are represented with blue and red balls, respectively.

butterfly-shaped U_2O_4 motif have recently been synthesized and characterized.[80] In the butterfly-shaped U_2O_4 core, one dioxouranium unit has been converted from the traditionally linear format to a bent/cis-like shape, Figure 6. To determine the effect of oxo-functionalization on the ability of dioxouranium complexes to form binuclear complexes with butterfly-shaped U_2O_4 cores, we consider the dimerization of $UO_2(OH)_2$, $UO_2(OH)_2^-$, and $OUOSiH_3(OH)_2$. The latter

dx.doi.org/10.1021/ic301762g | Inorg. Chem. 2013, 52, 245−257

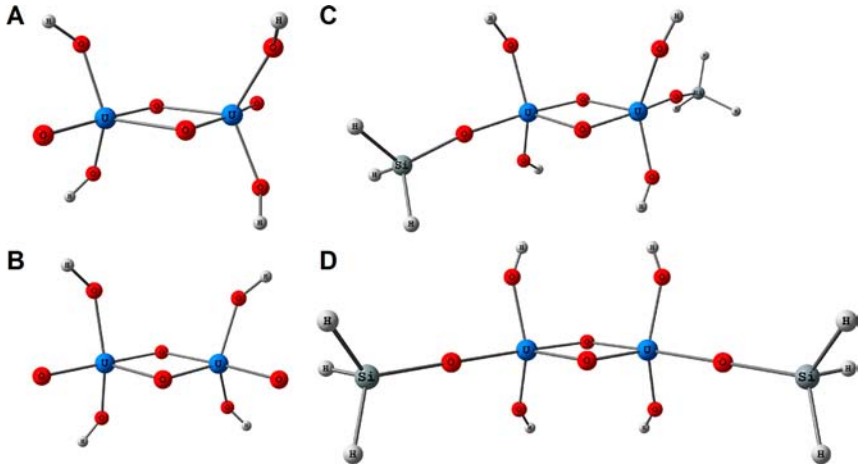

Figure 7. Dimers of $UO_2(OH)_2$ and $OUOSiH_3(OH)_2$ with diamond- and butterfly-shaped U_2O_4 cores. Structures with (A, C) diamond-shaped cores and (B, D) butterfly-shaped cores.

Table 7. Calculated Structural Parameters of the Dimers of $UO_2(OH)_2$, $UO_2(OH)_2^-$, and $OUOSiH_3(OH)_2$ Obtained at the B3LYP/B1 Level[a]

	U−O_{free}/U−$OSiH_3$	U−O	U−U
Diamond-U_2O_4			
$U_2O_4(OH)_4$	1.780 (2.42)	1.890/2.405 (1.83/0.50)	3.495
$U_2O_4(OH)_4^{2-}$	1.862 (2.37)	1.983/2.379 (1.70/0.65)	3.517
$(OUOSiH_3)_2(OH)_4$	2.081 (1.15)	2.070/2.141 (1.33/1.04)	3.388
Butterfly-U_2O_4			
$U_2O_4(OH)_4$	1.800 (2.44)	2.060−2.140 (1.12−1.24)	3.389
$U_2O_4(OH)_4^{2-}$	1.879 (2.39)	2.128/2.163 (1.16/1.17)	3.454
$(OUOSiH_3)_2(OH)_4$	2.079 (1.15)	2.108/2.100 (1.18/1.20)	3.389

[a]The Mayer bond orders obtained at the PBE/B2 level are given in parentheses.

two are the pentavalent and oxo-silylated pentavalent derivatives of $UO_2(OH)_2$, respectively. The ground-state structures of $U_2O_4(OH)_4$, the dimer of $UO_2(OH)_2$, and $(OUOSiH_3)_2(OH)_4$, the dimer of $OUOSiH_3(OH)_2$, possessing these two types of U_2O_4 cores are shown in Figure 7. Only the high-spin triplet states were considered for $U_2O_4(OH)_4^{2-}$ and $(OUOSiH_3)_2(OH)_4$ as a result of some spin contamination in their antiferromagnetically coupled singlet U(V)/U(V) states.

Energetically, the structure with a diamond-shaped U_2O_4 core in $U_2O_4(OH)_4$, Figure 7A, was found to be about 12.2 kcal/mol more stable than the structure with a butterfly-shaped U_2O_4 core, Figure 7B. For $U_2O_4(OH)_4^{2-}$, the dimer of $UO_2(OH)_2^-$, the energy difference between structures with these U_2O_4 cores was found to be 8.9 kcal/mol, also in favor of the diamond-shaped core. In contrast to the high energy differences between the structures with butterfly- and diamond-shaped cores in $U_2O_4(OH)_4$ and $U_2O_4(OH)_4^{2-}$, the energy difference between these structures of $(OUOSiH_3)_2(OH)_4$ was calculated to be about 0.9 kcal/mol. The structures with butterfly-shaped cores in $U_2O_4(OH)_4$, $U_2O_4(OH)_4^{2-}$, and $(OUOSiH_3)_2(OH)_4$ were all found to be local minima structures on their potential energy surfaces. The stability of the diamond U_2O_4 complexes relative to their counterparts with butterfly-shaped U_2O_4 cores follows the trend hexavalent > pentavalent ≫ oxo-functionalized pentavalent. This trend can be related to the structures of the binuclear complexes, especially the bond lengths and strengths of the U═O/U—O_{free} bonds not included in the U_2O_4 core. It is the bending of one of these bonds that confers the diamond or butterfly shape on the U_2O_4 core. As presented in Table 7, this bond is shortest in the hexavalent complex and longest in the oxo-functionalized dimer. The Mayer bond orders for these bonds also decrease from 2.42 to 2.37 and 1.12, respectively. The higher stability of the butterfly-shaped U_2O_4 core in the oxo-functionalized U(V)/U(V) dimer is a reflection of the ease with which the U—$OSiH_3$ bond can be bent in comparison to the triple U═O bonds in $U_2O_4(OH)_4$ and $U_2O_4(OH)_4^{2-}$. It is important to note the dimer species with diamond- and butterfly-shaped cores are not the most stable structures. The μ_2-dihydroxo (two bridging hydroxo ligands) structure, shown in the Supporting Information, of $U_2O_4(OH)_4$ is more stable than the structures with diamond-shaped (12.3 kcal/mol) or butterfly-shaped (24.5 kcal/mol) U_2O_4 cores. Similarly, in $(OUOSiH_3)_2(OH)_4$ and $U_2O_4(OH)_4^{2-}$, the diamond-shaped (2.0−4.5 kcal/mol) and butterfly-shaped (6.3−13.3 kcal/mol) structures are also less stable than the μ_2-dihydroxo structure. We have however focused on the structures with diamond- and butterfly-shaped cores, which are essentially high-lying minima, given their structural similarity to well-known dimeric and polymeric uranyl species held together by cation−cation interactions.[1,4,27,28]

There is a major difference in the nature of the U—O bonds found in the inner U_2O_2 units of the butterfly- and diamond-shaped U_2O_4 cores. In the complexes with diamond-shaped cores, each oxo atom of the U_2O_2 unit interacts with the adjacent uranium atom. This cation−cation interaction through the axial oxo atoms results in the existence of two types of bonds: a shorter U—O bond belonging to one dioxouranium unit and a longer U—O bond between the oxygen atom of one UO_2 unit and the uranium atom of another, Table 7. The short

dx.doi.org/10.1021/ic301762g | Inorg. Chem. 2013, 52, 245−257

Table 8. Calculated Mulliken (B3LYP/B1 Level) and Hirshfeld Partial Atomic Charges (PBE/B2 Level) Obtained for Several Hexavalent, Pentavalent, and Oxo-Functionalized Pentavalent Complexes

	B3LYP/B1			PBE/B2		
	U	$=O/O_{free}$	O_{func}	U	$=O/O_{free}$	O_{func}
Hexavalent						
UO_2^{2+}	1.98	0.01		2.10	−0.05	
$UO_2(H_2O)_5^{2+}$	1.66	−0.20		1.10	−0.21	
Pentavalent						
UO_2^{+}	1.47	−0.24		1.44	−0.22	
$UO_2(H_2O)_5^{+}$	1.39	−0.39		0.63	−0.32	
Oxo-Functionalized Pentavalent						
$OUOH^{2+}$	1.95	−0.06	−0.32	2.03	−0.09	−0.34
$OUO(SiH_3)^{2+}$	1.80	−0.11	−0.43	1.88	−0.13	−0.42
$OUOH(H_2O)_5^{2+}$	1.78	−0.26	−0.53	1.11	−0.23	−0.39
$OUO(SiH_3)(H_2O)_5^{2+}$	1.75	−0.28	−0.53	1.14	−0.25	−0.49

U—O bonds in the U_2O_2 units are longer than the free U=O bonds found in $U_2O_4(OH)_4$ and $U_2O_4(OH)_4^{2-}$, Figure 7. This is due to perturbation by adjacent uranium atoms. In the complexes with butterfly-shaped U_2O_4 cores however, the U—O bonds in the U_2O_2 unit are essentially within similar bond length ranges, Table 7. As previously noted, the origin of this similarity in the U—O bond lengths found in the U_2O_2 unit of butterfly U_2O_4 complexes is related to their O—U—O—U—O nature.[80] In essence, the oxo atoms in the U_2O_2 unit are now oxide bridges, rather than cation−cation interactions, between two uranium oxide units.

We note that the target complexes studied in this section contain equatorial hydroxo ligands. The motivations behind the selection of these target complexes are 2-fold. For the first part (Section 3.3.1), it is far easier for the hydroxo ligand to form a *cis*-uranyl type complex than the aquo ligands found in the complexes studied in the previous section.[7,41,52] Second, the use of the neutral $UO_2(OH)_2$ species in the study of the dimerization (Section 3.3.2) allows us to minimize the impact of repulsive electrostatic interactions. This isolates the effects of oxo-functionalization on going from $U_2O_4(OH)_4$ to $(OUOSiH_3)_2(OH)_4$. The stability of the butterfly U_2O_4 core after oxo-functionalization also extends to other equatorial ligands (Supporting Information, Table S1 and Scheme S1).

3.4. Atomic Charges. The calculated Mulliken atomic partial charges in several hexavalent uranyl complexes and their pentavalent oxo-functionalized derivatives are compiled in Table 8. These values were obtained at the B3LYP/B1 and PBE/B2 levels. The issues afflicting the Mulliken population analysis method include its tendency toward overestimating bond covalency and basis set dependence. The trend in the calculated charges should however afford us a qualitative picture of the charge distributions in these molecules. The calculated charge distribution indicate that the oxo atoms of UO_2^{+} and $UO_2(H_2O)_5^{+}$ are significantly more electronegative than those found in UO_2^{2+} and $UO_2(H_2O)_5^{2+}$. A similar phenomenon is observed for the free oxo atoms in the pentavalent oxo-functionalized complexes, Table 8. For example, the calculated Mulliken charge on the oxo atoms in UO_2^{2+} is 0.01 while the charges on the free oxo atoms of $OUOH^{2+}$ and $OUO(SiH_3)^{2+}$ are −0.06 and −0.11, respectively. The free oxo atoms in the oxo-functionalized complexes are however less basic (Lewis definition) than those found in the UO_2^{+} and $UO_2(H_2O)_5^{+}$. Overall, one expects that the free oxo atoms in the oxo-functionalized pentavalent complexes would be more susceptible to attack by electropositive reagents than those in the hexavalent species, albeit to a lesser extent than the oxo atoms of UO_2^{+} and $UO_2(H_2O)_5^{+}$.

3.5. Implications of the Charge Distribution in Oxo-Functionalized Complexes. *3.5.1. Interaction with Electropositive Reagents.* The dimerization of $UO_2(OH)_2$, $UO_2(OH)_2^{-}$, and $OUOSiH_3(OH)_2$ to give dimers with diamond-shaped U_2O_4 cores can provide insights into the relative susceptibility of the free oxo atoms to attack by electropositive reagents. This is because the UO_2 monomers in the diamond U_2O_4 dimers are essentially held together by cation−cation interactions between the free oxo atoms of the monomers and the uranium atom of the adjacent monomer. The energy of formation of the $U_2O_4(OH)_4$, $U_2O_4(OH)_4^{2-}$, and $(OUOSiH_3)_2(OH)_4$ complexes with diamond cores from their respective monomeric species were calculated as −33.60, 2.83, and −50.21 kcal/mol, respectively, at the B3LYP/B2 level. The dimerization of $(OUOSiH_3)_2(OH)_4$ is significantly more exothermic than those of $U_2O_4(OH)_4$ and $U_2O_4(OH)_4^{2-}$. The free axial oxo atoms in $UO_2(OH)_2$, $UO_2(OH)_2^{-}$, and $OUOSiH_3(OH)_2$ have charges of −0.322, −0.530, and −0.383, respectively, while the uranium centers have charges of 1.279, 1.095, and 1.274, respectively. The extra density on the free oxo atom of the silylated complex allows for stronger cation−cation interactions in its dimer in comparison to its hexavalent counterpart. On the other hand, the weak exothermicity obtained for the dimerization of $UO_2(OH)_2^{-}$ is most likely a reflection of electrostatic repulsion.

A similar example to this can be demonstrated by examining the coordination of $B(CH_3)_3$ to the axial oxo atoms of $UO_2(OCH_3)_2$, $UO_2(OCH_3)_2^{-}$, and $OUOSiH_3(OCH_3)_2$. We have used equatorial methoxy groups rather than hydroxo groups to prevent interaction with the incoming $B(CH_3)_3$ ligand. In the aggregate complexes, $(CH_3)_3BOUO(OCH_3)_2^{-}$ and $(CH_3)_3BOUOSiH_3(OCH_3)_2$, the O−B bond lengths were calculated to be 1.552 and 1.626 Å, respectively, at the B3LYP/B1 level. The hexavalent complex, $(CH_3)_3BOUO(OCH_3)_2$, essentially broke apart at the B3LYP/B1 level in the gas phase. The oxo atom in $UO_2(OCH_3)_2^{-}$ and the free oxo atom in $OUOSiH_3(OCH_3)_2$ simply have greater electron densities for contribution to the incoming electrophile. The polarizability of the U−O bonds in $UO_2(OCH_3)_2^{-}$ and $OUOSiH_3(OCH_3)_2$ might be another contributing factor to this effect.

3.5.2. U(V)−U(IV) Redox Potentials. The calculated atomic charges, Table 8, indicate that the uranium centers in the oxo-functionalized pentavalent complexes are significantly more positively charged than those of UO_2^{+} and $UO_2(H_2O)_5^{+}$. This

dx.doi.org/10.1021/ic301762g | Inorg. Chem. 2013, 52, 245−257

goes back to the fact that, although reductive oxo-functionalization creates a U(V) center, the overall charge of the molecule remains unchanged. From the calculated charges, it appears that it would be easier to add an electron to (higher electron affinity) and more difficult to remove an electron from (higher ionization potentials) the U(V) centers of the oxo-functionalized pentavalent complexes. The higher atomic charges on these centers indicate lower electron densities in comparison to those of UO_2^+ and $UO_2(H_2O)^{5+}$.

To examine the effect of oxo-silylation on the U(V)−U(IV) redox potential, we have optimized the structures of $UO_2(Py)(H_2L)^-$ and $OUOSiH_3(Py)(H_2L)$, where Py is pyridine, and calculated their vertical reduction potentials after optimizing the geometries of their U(IV) analogues. In these complexes, the H_4L ligand is a Pacman-type organic ligand that possesses four amine (NH) sites. In $UO_2(Py)(H_2L)^-$, two of the centers have been transaminated by the uranyl ligand.[14] The reduction of $UO_2(Py)(H_2L)^-$ and $OUOSiH_3(Py)(H_2L)$ to the +4 oxidation state is considered in tetrahydrofuran (THF) rather than the aqueous reduction of $UO_2(H_2O)_5^+$ and $OUO(SiH_3)(H_2O)_5^{2+}$.

The U(V)/U(IV) reduction potentials of $UO_2(Py)(H_2L)^-$ and $OUOSiH_3(Py)(H_2L)$ were calculated to be −3.20 and −1.75 eV, respectively, against the ferrocene/ferrocenium electrode. After the inclusion of the Hay corrections, about 0.31 eV, these values were shifted to −2.89 and −1.44 eV, respectively.[81] The Hay correction accounts for multiplet and spin−orbit coupling effects that exist in the actual systems but are lacking in scalar relativistic DFT calculations. As expected, as a result of the higher electron density on its U(V) center, it is more difficult to reduce $UO_2(Py)(H_2L)^-$ than to reduce $OUOSiH_3(Py)(H_2L)$. Oxo-functionalization lowers the electron density at the actinide center thereby lowering its reduction potential. We have used the organic Pacman ligand as well as THF solvent in order to bypass the formation of $U(H_2O)_8^{4+}$ in aqueous solutions and the relative "ambiguity" of the reactions:

$$UO_2(H_2O)_5^+ + 4H_3O^+ + e^- \rightarrow U(H_2O)_8^{4+} + 3H_2O$$

$$OUO(SiH_3)(H_2O)_5^{2+} + 4H_3O^+ + e^- \rightarrow U(H_2O)_8^{4+} + 3H_2O + SiH_3^+$$

The U(V)/U(IV) reduction potentials of $UO_2(H_2O)_5^{2+}$ and $OUO(SiH_3)(H_2O)_5^{2+}$ according to the above reactions were calculated as −3.06 and −0.35 eV relative to the ferrocene/ferrocenium electrode. Although this follows the same trend as observed for the Pacman complexes, the reaction written for the reduction of the silylated pentaaquo complex in aqueous solution should be taken with care.

It is important to mention that Schnaars et al. have indeed shown that oxo-functionalization with $B(C_6F_5)_3$ facilitates the reduction of the pentavalent complex $[Cp^*_2Co][U(V)O_2(^{Ar}acnac)_2]$, (where Ar is 3,5-$^tBu_2C_6H_3$), to the tetravalent state.[82] They postulated that the $B(C_6F_5)_3$ axial group actually shifts the reduction process to a point where it is chemically accessible (against the ferrocene/ferrocenium electrode). A similar effect has been observed for the U(VI)/U(V) reduction of an hexavalent complex, $UO_2(^{Ar}acnac)_2$, and its axially oxo-functionalized hexavalent counterpart, $OUOB(C_6F_5)_3(^{Ar}acnac)_2$.[16] In a similar manner, some electron density from the uranyl U═O bond in $UO_2(^{Ar}acnac)_2$ is transferred to the axial $B(C_6F_5)_3$ ligand in $OUOB(C_6F_5)_3(^{Ar}acnac)_2$. The lower electron density on the U(VI) center in $OUOB(C_6F_5)_3(^{Ar}acnac)_2$ results in a lower reduction potential of −0.78 V compared to a value of −1.52 V for $UO_2(^{Ar}acnac)_2$.

4. CONCLUSIONS

In this work, we have studied the structural and electronic properties of model oxo-functionalized (oxo-protonated and oxo-silylated) pentavalent dioxouranium complexes using scalar relativistic DFT calculations. Their structures and properties are compared to those of their hexavalent and pentavalent counterparts with free oxo atoms. Particular emphasis was placed on the effect of their electronic structures on the formation of cation−cation complexes, the type of U_2O_4 core in the binuclear complexes they form, as well as the effect on the U(V)/U(IV) redox potentials.

The electronic structures of the oxo-protonated and oxo-silylated pentavalent complexes are different from those of their hexavalent and pentavalent counterparts with free oxo atoms with respect to the stabilization of the UO_2 σ(d) orbitals. The axial nature of OH and $OSiH_3$ groups in the oxo-functionalized complexes allows for mixing of the uranyl σ(d) orbital with the more stable σ(OH)/σ($OSiH_3$) orbitals. This is somewhat reminiscent of the stabilization of the actinyl σ(d) orbital on coordination of an equatorial hydroxo or siloxo group. As a result of this stabilization, the participation of the 6p orbitals in the σ(d) orbitals of the oxo-functionalized pentavalent complexes exceed those of their counterparts with free oxo groups.

The major structural effect of reductively protonating or silylating an oxo atom of the uranyl moiety is the significant weakening of the bond between the uranium center and the functionalized oxo atom. The U═O bond in the uranyl group is elongated by up to 0.24 Å in forming the U—OH/U—$OSiH_3$ bond. In contrast, the bond between the uranium atom and the free oxo atom, $U—O_{free}$ bonds, in the oxo-functionalized complexes is only weakened by about 0.01−0.03 Å. The inherent asymmetry in these complexes is reflected in the atomic contributions to the valence orbitals of the dioxouranium units. Examination of the calculated bond orders and the electronic structure indicates that, while oxo-functionalization leads to the loss of a full bond order for the $U—O_{func}$ bonds, there is actually a slight increase in the covalency of the other axial bond, the $U—O_{free}$ bonds. This was found to be due to the increased O-2p contributions from the free oxo atom as well as higher U-5f contributions to the σ(f) and π(f) orbitals.

Interestingly, the calculated bond orders indicated that, after oxo-functionalization, the axial U—OH/U—$OSiH_3$ bonds are only slightly stronger than their equatorial counterparts. This opens the way for ligand exchange between axial U—O bonds and their equatorial counterparts. An example involving exchange between conformers with either an axial(/equatorial) U—OH bond and an equatorial(/axial) U—$OSiH_3$ bond was found to favor the conformer with an axial U—OH bond and equatorial U—$OSiH_3$ bond combination by about 3.90 kcal/mol. This is significantly less than the approximately 17.3 kcal/mol needed to exchange the axial oxo group with the equatorial OH group of $UO_2(OH)_4^{2-}$. The possibility of having two or more conformers corresponding to an exchange reaction between axial groups (formed by oxo-functionalization) and equatorial groups sheds light on some recent experimental reports. A related effect to this is found in the energy differences between binuclear complexes with butterfly- or

dx.doi.org/10.1021/ic301762g | Inorg. Chem. 2013, 52, 245−257

diamond-shaped U_2O_4 cores. The fact that the axial U—O_{func} bonds in the oxo-functionalized complexes are far weaker than the U═O bonds in their hexavalent and pentavalent counterparts implies that it is easier to bend these bonds in converting the diamond U_2O_4 core into a butterfly format.

The charge distributions on the uranium and oxo atoms in the oxo-functionalized pentavalent complexes are more conducive to formation of binuclear complexes held together by cation−cation interactions than their hexavalent counterparts. This is due to the presence of extra electron density on the free oxo atom in these O═U—OX complexes. Another effect of the charge distributions on these complexes was found in the U(V)/U(IV) redox potentials. Reductive oxo-functionalization depletes the charge on the uranium centers, in comparison to pentavalent complexes with free oxo atoms. The implication of this is that the uranium centers in the oxo-functionalized pentavalent complexes are more receptive toward an incoming electron, thereby shifting their U(V)/U(IV) redox potentials significantly into a chemically accessible range.

Overall, we have compared the electronic structures of oxo-functionalized pentavalent dioxouranium complexes to those of UO_2^{2+} and UO_2^{+} species using theoretical calculations. The effects of their electronic structures on their chemical and structural properties were also examined. The trend observed for the select model complexes is transferrable to uranyl complexes formed with other ligands. This work is in line with our research theme of understanding the U(VI)/U(V)/U(IV) reduction processes as it pertains to controlling the migration of radionuclides in the natural environment.

■ ASSOCIATED CONTENT

Ⓢ Supporting Information

Structures of the uranyl Pacman complex, $UO_2(py)(H_2L)$, and its oxo-functionalized pentavalent derivatives optimized at the B3LYP/B1 level; supplement to Figure 2 of the main manuscript: the actual energies of the HOMOs in several uranyl species; a table of the calculated reaction free energies ($\Delta G298$, kcal/mol) required to transaminate the unoccupied amine site of several Pacman complexes with a *cis*-uranyl group; a scheme showing insertion of a cis-type UO_2 group into uranyl Pacman complexes; and the μ2-dihydroxo structure of $(UO_2)_2(OH)_4$ optimized at the B3LYP/B1 level. This material is available free of charge via the Internet at http://pubs.acs.org.

■ AUTHOR INFORMATION

Corresponding Author

*E-mail: schrecke@cc.umanitoba.ca.

Notes

The authors declare no competing financial interest.

■ ACKNOWLEDGMENTS

The authors are grateful to Polly Arnold and Jason Love for helpful discussions. S.O.O. gratefully thanks the Provincial Government of Manitoba, Canada, for partial funding for this project via the Manitoba Graduate Scholarship. He is also grateful to the Faculty of Graduate Studies at the University of Manitoba for financial assistance through the University of Manitoba Graduate Fellowship (UMGF). G.S. acknowledges financial support from the Natural Sciences and Engineering Research Council of Canada (NSERC). The Grex cluster of the Western Canada Research Grid (WestGrid) was used for some of the computations in this work.

■ REFERENCES

(1) Arnold, P. L.; Love, J. B.; Patel, D. *Coord. Chem. Rev.* **2009**, *253*, 1973.
(2) Ephritikhine, M. *Dalton Trans.* **2006**, 2501.
(3) Fortier, S.; Hayton, T. W. *Coord. Chem. Rev.* **2010**, *254*, 197.
(4) Graves, C. R.; Kiplinger, J. L. *Chem. Commun.* **2009**, 3831.
(5) Melfi, P. J.; Kim, S. K.; Lee, J. T.; Bolze, F.; Seidel, D.; Lynch, V. M.; Veauthier, J. M.; Gaunt, A. J.; Neu, M. P.; Ou, Z.; Kadish, K. M.; Fukuzumi, S.; Ohkubo, K.; Sessler, J. L. *Inorg. Chem.* **2007**, *46*, 5143.
(6) Pan, Q. J.; Schreckenbach, G. *Inorg. Chem.* **2010**, *49*, 6509.
(7) Schreckenbach, G.; Shamov, G. A. *Acc. Chem. Res.* **2010**, *43*, 19.
(8) Sessler, J. L.; Gorden, A. E. V.; Seidel, D.; Hannah, S.; Lynch, V.; Gordon, P. L.; Donohoe, R. J.; Tait, C. D.; Keogh, D. W. *Inorg. Chim. Acta* **2002**, *341*, 54.
(9) Sessler, J. L.; Melfi, P. J.; Pantos, G. D. *Coord. Chem. Rev.* **2006**, *250*, 816.
(10) Sessler, J. L.; Vivian, A. E.; Seidel, D.; Burrell, A. K.; Hoehner, M.; Mody, T. D.; Gebauer, A.; Weghorn, S. J.; Lynch, V. *Coord. Chem. Rev.* **2001**, *216*, 411.
(11) Burns, C. J.; Clark, D. L.; Donohoe, R. J.; Duval, P. B.; Scott, B. L.; Tait, C. D. *Inorg. Chem.* **2000**, *39*, 5464.
(12) Arnold, P. L.; Patel, D.; Blake, A. J.; Wilson, C.; Love, J. B. *J. Am. Chem. Soc.* **2006**, *128*, 9610.
(13) Sarsfield, M. J.; Helliwell, M. *J. Am. Chem. Soc.* **2004**, *126*, 1036.
(14) Arnold, P. L.; Blake, A. J.; Wilson, C.; Love, J. B. *Inorg. Chem.* **2004**, *43*, 8206.
(15) Arnold, P. L.; Pecharman, A. F.; Hollis, E.; Yahia, A.; Maron, L.; Parsons, S.; Love, J. B. *Nat. Chem.* **2010**, *2*, 1056.
(16) Hayton, T. W.; Wu, G. *Inorg. Chem.* **2009**, *48*, 3065.
(17) Ikeda, A.; Hennig, C.; Tsushima, S.; Takao, K.; Ikeda, Y.; Scheinost, A. C.; Bernhard, G. *Inorg. Chem.* **2007**, *46*, 4212.
(18) Mizuoka, K.; Grenthe, I.; Ikeda, Y. *Inorg. Chem.* **2005**, *44*, 4472.
(19) Mizuoka, K.; Ikeda, Y. *Inorg. Chem.* **2003**, *42*, 3396.
(20) Mizuoka, K.; Ikeda, Y. *Radiochem. Acta* **2004**, *92*, 631.
(21) Mizuoka, K.; Kim, S. Y.; Hasegawa, M.; Hoshi, T.; Uchiyama, G.; Ikeda, Y. *Inorg. Chem.* **2003**, *42*, 1031.
(22) Berthet, J. C.; Nierlich, M.; Ephritikhine, M. *Angew. Chem., Int. Ed.* **2003**, *42*, 1952.
(23) Burdet, F.; Pecaut, J.; Mazzanti, M. *J. Am. Chem. Soc.* **2006**, *128*, 16512.
(24) Mougel, V.; Horeglad, P.; Nocton, G.; Pecaut, J.; Mazzanti, M. *Angew. Chem., Int. Ed.* **2009**, *48*, 8477.
(25) Mougel, V.; Horeglad, P.; Nocton, G.; Pecaut, J.; Mazzanti, M. *Chem.—Eur. J.* **2010**, *16*, 14365.
(26) Natrajan, L.; Burdet, F.; Pecaut, J.; Mazzanti, M. *J. Am. Chem. Soc.* **2006**, *128*, 7152.
(27) Nocton, G.; Horeglad, P.; Pecaut, J.; Mazzanti, M. *J. Am. Chem. Soc.* **2008**, *130*, 16633.
(28) Nocton, G.; Horeglad, P.; Vetere, V.; Pecaut, J.; Dubois, L.; Maldivi, P.; Edelstein, N. M.; Mazzanti, M. *J. Am. Chem. Soc.* **2010**, *132*, 495.
(29) Arnold, P. L.; Patel, D.; Wilson, C.; Love, J. B. *Nature* **2008**, *451*, 315.
(30) Arnold, P. L.; Pecharman, A.-F.; Love, J. B. *Angew. Chem., Int. Ed.* **2011**, *50*, 9456.
(31) Schnaars, D. D.; Wu, G.; Hayton, T. W. *Inorg. Chem.* **2011**, *50*, 9642.
(32) Schnaars, D. D.; Wu, G.; Hayton, T. W. *Inorg. Chem.* **2011**, *50*, 4695.
(33) Arnold, P. L.; Holis, E.; Nichol, G. S.; Love, J. B.; Griveau, J. C.; Caciuffo, R.; Magnani, N.; Maron, L.; Castro, L.; Yahia, A.; Odoh, S. O.; Schreckenbach, G. J. *J. Am. Chem. Soc.* **2013**, submitted.
(34) Arnold, P. L.; Hollis, E.; White, F. J.; Magnani, N.; Caciuffo, R.; Love, J. B. *Angew. Chem., Int. Ed.* **2011**, *50*, 887.
(35) Berthet, J. C.; Siffredi, G.; Thuery, P.; Ephritikhine, M. *Chem. Commun.* **2006**, 3184.

(36) Austin, J. P.; Sundararajan, M.; Vincent, M. A.; Hillier, I. H. *Dalton Trans.* **2009**, 5902.
(37) Batista, E. R.; Martin, R. L.; Hay, P. J. *J. Phys. Chem.* **2004**, *121*, 11104.
(38) de Jong, W. A.; Apra, E.; Windus, T. L.; Nichols, J. A.; Harrison, R. J.; Gutowski, K. E.; Dixon, D. A. *J. Phys. Chem. A* **2005**, *109*, 11568.
(39) de Jong, W. A.; Harrison, R. J.; Nichols, J. A.; Dixon, D. A. *Theor. Chem. Acc.* **2001**, *107*, 22.
(40) Garcia-Hernandez, M.; Lauterbach, C.; Krüger, S.; Matveev, A.; Rösch, N. *J. Comput. Chem.* **2002**, *23*, 834.
(41) Garcia-Hernandez, M.; Willnauer, C.; Krüger, S.; Moskaleva, L. V.; Rosch, N. *Inorg. Chem.* **2006**, *45*, 1356.
(42) Han, Y. K. *J. Comput. Chem.* **2001**, *22*, 2010.
(43) Han, Y. K.; Hirao, K. *J. Phys. Chem.* **2000**, *113*, 7345.
(44) Hay, P. J.; Martin, R. L. *J. Phys. Chem.* **1998**, *109*, 3875.
(45) Ingram, K. I. M.; Haller, L. J. L.; Kaltsoyannis, N. *Dalton Trans.* **2006**, 2403.
(46) Odoh, S. O.; Pan, Q. J.; Shamov, G. A.; Wang, F. Y.; Fayek, M.; Schreckenbach, G. *Chem.—Eur. J.* **2012**, *18*, 7117.
(47) Odoh, S. O.; Reyes, J. A.; Schreckenbach, G. *Inorg. Chem.* **2013**, submitted for publication.
(48) Odoh, S. O.; Schreckenbach, G. *J. Phys. Chem. A* **2010**, *114*, 1957.
(49) Odoh, S. O.; Schreckenbach, G. *J. Phys. Chem. A* **2011**, *115*, 14110.
(50) Odoh, S. O.; Walker, S. M.; Meier, M.; Stetefeld, J.; Schreckenbach, G. *Inorg. Chem.* **2011**, *50*, 3141.
(51) Schlosser, F.; Moskaleva, L. V.; Kremleva, A.; Krüger, S.; Rösch, N. *Dalton Trans.* **2010**, *39*, 5705.
(52) Schreckenbach, G.; Hay, P. J.; Martin, R. L. *Inorg. Chem.* **1998**, *37*, 4442.
(53) Schreckenbach, G.; Hay, P. J.; Martin, R. L. *J. Comput. Chem.* **1999**, *20*, 70.
(54) Shamov, G. A.; Schreckenbach, G. *J. Phys. Chem. A* **2005**, *109*, 10961. Shamov, G. A.; Schrekenbach, G. *J. Phys. Chem. A* **2006**, *110*, 12072.
(55) Shamov, G. A.; Schreckenbach, G.; Vo, T. N. *Chem.—Eur. J.* **2007**, *13*, 4932.
(56) Tsushima, S.; Uchida, Y.; Reich, T. *Chem. Phys. Lett.* **2002**, *357*, 73.
(57) Vallet, V.; Macak, P.; Wahlgren, U.; Grenthe, I. *Theor. Chem. Acc.* **2006**, *115*, 145.
(58) Vlaisavljevich, B.; Gagliardi, L.; Burns, P. C. *J. Am. Chem. Soc.* **2010**, *132*, 14503.
(59) Vukovic, S.; Watson, L. A.; Kang, S. O.; Custelcean, R.; Hay, B. P. *Inorg. Chem.* **2012**, *51*, 3855.
(60) Kaltsoyannis, N.; Hay, P. J.; Li, J.; Blaudeau, J. P.; Bursten, B. E. Theoretical studies of the electronic structure of compounds of the actinides. In *The Chemistry of the Actinide and Transactinide Elements*, 3rd ed.; Springer: Dordrecht, The Netherlands, 2006; Vol. *3*.
(61) Denning, R. G. *J. Phys. Chem. A* **2007**, *111*, 4125.
(62) Denning, R. G. *Struct. Bonding (Berlin, Ger.)* **1992**, *79*, 215.
(63) Moskaleva, L. V.; Krüger, S.; Spörl, A.; Rösch, N. *Inorg. Chem.* **2004**, *43*, 4080.
(64) Tsushima, S. *Inorg. Chem.* **2009**, *48*, 4856.
(65) Vallet, V.; Maron, L.; Schimmelpfennig, B.; Leininger, T.; Teichteil, C.; Gropen, O.; Grenthe, I.; Wahlgren, U. *J. Phys. Chem. A* **1999**, *103*, 9285.
(66) Vallet, V.; Schimmelpfennig, B.; Maron, L.; Teichteil, C.; Leininger, T.; Gropen, O.; Grenthe, I.; Wahlgren, U. *Chem. Phys.* **1999**, *244*, 185.
(67) Wang, X. F.; Andrews, L.; Vlaisavljevich, B.; Gagliardi, L. *Inorg. Chem.* **2011**, *50*, 3826.
(68) Frisch, M. J.; Trucks, G. W.; Schlegel, H. B.; Scuseria, G. E.; Robb, M. A.; Cheeseman, J. R.; Montgomery, Jr., J. A.; Vreven, T.; Kudin, K. N.; Burant, J. C.; Millam, J. M.; Iyengar, S. S.; Tomasi, J.; Barone, V.; Mennucci, B.; Cossi, M.; Scalmani, G.; Rega, N.; Petersson, G. A.; Nakatsuji, H.; Hada, M.; Ehara, M.; Toyota, K.; Fukuda, R.; Hasegawa, J.; Ishida, M.; Nakajima, T.; Honda, Y.; Kitao, O.; Nakai, H.; Klene, M.; Li, X.; Knox, J. E.; Hratchian, H. P.; Cross, J. B.; Bakken, V.; Adamo, C.; Jaramillo, J.; Gomperts, R.; Stratmann, R. E.; Yazyev, O.; Austin, A. J.; Cammi, R.; Pomelli, C.; Ochterski, J. W.; Ayala, P. Y.; Morokuma, K.; Voth, G. A.; Salvador, P.; Dannenberg, J. J.; Zakrzewski, V. G.; Dapprich, S.; Daniels, A. D.; Strain, M. C.; Farkas, O.; Malick, D. K.; Rabuck, A. D.; Raghavachari, K.; Foresman, J. B.; Ortiz, J. V.; Cui, Q.; Baboul, A. G.; Clifford, S.; Cioslowski, J.; Stefanov, B. B.; Liu, G.; Liashenko, A.; Piskorz, P.; Komaromi, I.; Martin, R. L.; Fox, D. J.; Keith, T.; Al-Laham, M. A.; Peng, C. Y.; Nanayakkara, A.; Challacombe, M.; Gill, P. M. W.; Johnson, B.; Chen, W.; Wong, M. W.; Gonzalez, C.; Pople, J. A. *Gaussian 03*, Revision C.02; Gaussian, Inc.: Wallingford, CT, 2004.
(69) Laikov, D. N. *Chem. Phys. Lett.* **2005**, *416*, 116.
(70) Laikov, D. N.; Ustynyuk, Y. A. *Russ. Chem. Bull.* **2005**, *54*, 820.
(71) Küchle, W.; Dolg, M.; Stoll, H.; Preuss, H. *Mol. Phys.* **1991**, *74*, 1245.
(72) Küchle, W.; Dolg, M.; Stoll, H.; Preuss, H. *J. Phys. Chem.* **1994**, *100*, 7535.
(73) Schäfer, A.; Huber, C.; Ahlrichs, R. *J. Chem. Phys.* **1994**, *100*, 5829.
(74) Tomasi, J.; Mennucci, B.; Cammi, R. *Chem. Rev.* **2005**, *105*, 2999.
(75) Bridgeman, A. J.; Cavigliasso, G.; Ireland, L. R.; Rothery, J. *J. Chem. Soc., Dalton Trans.* **2001**, 2095.
(76) Clark, D. L.; Hobart, D. E.; Neu, M. P. *Chem. Rev.* **1995**, *95*, 25.
(77) Vallet, V.; Wahlgren, U.; Schimmelpfennig, B.; Moll, H.; Szabo, Z.; Grenthe, I. *Inorg. Chem.* **2001**, *40*, 3516.
(78) Clark, D. L.; Conradson, S. D.; Donohoe, R. J.; Keogh, D. W.; Morris, D. E.; Palmer, P. D.; Rogers, R. D.; Tait, C. D. *Inorg. Chem.* **1999**, *38*, 1456.
(79) Szabo, Z.; Grenthe, I. *Inorg. Chem.* **2010**, *49*, 4928.
(80) Arnold, P. L.; Jones, G. M.; Odoh, S. O.; Schreckenbach, G.; Magnani, N.; Love, J. B. *Nat. Chem.* **2012**, *4*, 221.
(81) Hay, P. J.; Martin, R. L.; Schreckenbach, G. *J. Phys. Chem. A* **2000**, *104*, 6259.
(82) Schnaars, D. D.; Wu, G.; Hayton, T. W. *J. Am. Chem. Soc.* **2009**, *131*, 17532.
(83) Allen, P. G.; Bucher, J. J.; Shuh, D. K.; Edelstein, N. M.; Reich, T. *Inorg. Chem.* **1997**, *36*, 4676.
(84) Jones, L. H.; Penneman, R. A. *J. Phys. Chem.* **1953**, *21*, 542.
(85) Toth, L. M.; Begun, G. M. *J. Phys. Chem.* **1981**, *85*, 547.